Contract No:

This document was prepared in conjunction with work accomplished under Contract No. 89303321CEM000080 with the U.S. Department of Energy (DOE) Office of Environmental Management (EM).

Disclaimer:

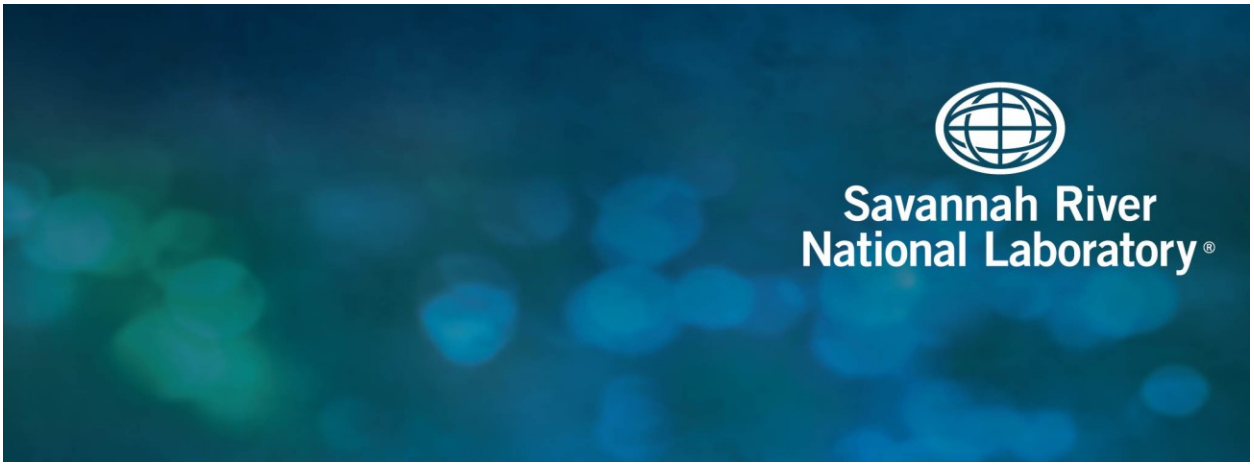

A U.S. DEPARTMENT OF ENERGY NATIONAL LAB • SAVANNAH RIVER SITE • AIKEN, SC • USA

FY21 Progress Report: 3013 Inner Container Closure Weld Region (ICCWR) Characterization by Wide Area 3D Measurement System (WAMS) Analysis

Emmanuel Perez

April 2022

SRNL-STI-2022-00063, Revision 0

DISCLAIMER

Printed in the United States of America

Prepared for
U.S. Department of Energy

SRNL-STI-2022-00063
Revision 0

Keywords: *3013, ICCWR, WAMS, characterization, report*

Retention: *Permanent*

FY21 Progress Report: 3013 Inner Container Closure Weld Region (ICCWR) Characterization by Wide Area 3D Measurement System (WAMS) Analysis

Emmanuel Perez

April 2022

Savannah River National Laboratory is operated by Battelle Savannah River Alliance for the U.S. Department of Energy under Contract No. 89303321CEM000080.

REVIEWS AND APPROVALS

AUTHORS:

_____

Emmanuel Perez, Advanced & Energy Materials Date

TECHNICAL REVIEW:

_____

Michael J. Martínez-Rodríguez, Tritium Technology, Reviewed per E7 2.60 Date

APPROVAL:

_____

Roderick Fuentes, Pu Surveillance Program Lead and Date
SRNL 3013 Surveillance Program Authority, Separation Sciences &Engineering

_____

Marissa Reigel, Manager Separation Sciences & Engineering Date

_____

Frank Pennebaker, Director Chemical Processing & Characterization Date

EXECUTIVE SUMMARY

As part of the 3013 Surveillance Program, through-wall penetration from stress corrosion cracking (SCC) of the 3013 inner containers has been identified as the most credible condition for failure withing the 50-years lifetime. Chlorides contained in Pu-bearing material, together with intra-canister humidity levels, metallurgical conditions, and internal stresses have been found to produce corrosion in the Inner Container Closure Weld Region (ICCWR) of the 3013 canister system. A Laser Confocal Microscope (LCM) is used as part of the 3013 Surveillance Program protocol to identify the prevalence of corrosion and corrosion-related cracking in the ICCWR2. With the LCM, a close visual examination is made of the ICCWR surface along with measurements of corrosion-related features. LCM inspections produce immense amounts of image data that is time intensive to analyze. There is also a 9-year backlog of images, with approximately 49 canisters that must be evaluated.

To expedite data analysis and reduce the amount of generated data, a Wide Area 3D Measurement System (WAMS) microscope has been added to the examination protocol. Although WAMS is a lower resolution microscope, small features of interest can be still identified. The advantage of collecting data for the full circumference using the WAMS is that it can take about 1/16 of the time needed with the LCM. Both systems offer capabilities that combined can be utilized to expedite the examination of the ICCWR. The WAMS is an efficient system for screening and identification of corrosion features while the LCM can be utilized to obtain higher resolution images areas identified by the WAMS.

This report explains and justifies the data collection methods used with the WAMS. It includes a summary of the data generated by WAMS in FY21. The goals set for data collection in FY21 were met. A total of twenty-two DE's were imaged, and analysis was carried out on eleven samples. The analyzed samples showed large numbers of potential cracks and pits distributed throughout the surfaces. Lastly, to explain the advantages of the WAMS, its capabilities were compared to those of a simpler microscope. Micrographs of the samples imaged in FY21 and those analyzed are included in the appendices.

TABLE OF CONTENTS

LIST OF TABLES

LIST OF FIGURES

LIST OF ABBREVIATIONS

SRNL	Savannah River National Laboratory
DE	Destructive Examination
DLE	Dino-Lite Edge digital microscope
EDS	Energy Dispersive Spectroscopy
FY	Fiscal Year
HHMC	Handford High Moisture Container
ICCWR	Inner Container Closure Weld Region
LANL	Los Alamos National Laboratory
LCM	Laser Confocal Microscope
LED	Light Emitting Diode
MIS	Materials Identification and Surveillance
MP	Megapixels
SEM	Scanning Electron Microscope, Scanning Electron Microscopy
SCC	Stress Corrosion Cracking, Stress Corrosion Crack
WAMS	Wide Area 3D Measurement System

1.0 Introduction

Through-wall penetration from stress corrosion cracking (SCC) of the 3013 inner containers has been identified as the most credible condition for failure withing the 50-years lifetime [1]. Chlorides contained in Pu-bearing material, together with intra-canister humidity levels, metallurgical conditions, and internal stresses have been found to produce corrosion in the Inner Container Closure Weld Region (ICCWR) of the 3013 canister system, which is used throughout the DOE complex. A Laser Confocal Microscope (LCM) is used as part of the 3013 Surveillance Program protocol to identify the prevalence of corrosion and corrosion-related cracking in the ICCWR. With the LCM, a close visual examination is made of the ICCWR surface along with measurements of corrosion-related features [2]. LCM inspections produce immense amounts of image data: approximately 6000 images per can, having 786,432 pixels per image, with 8 layers of data for each pixel. As FY21, there is a 9-year backlog of images, with approximately 49 canisters that must be evaluated.

To expedite data analysis and reduce the amount of generated data, a Wide Area 3D Measurement System (WAMS) microscope has been added to the examination protocol. Although the images from the LCM show higher resolution than those from the WAMS, small features of interest may be still identified. The advantage of collecting data for the full circumference using the WAMS is that it can take about a week to complete, which represents 1/16 of the time needed with the LCM. Nonetheless, both systems offer capabilities that combined can be utilized to expedite the examination of the ICCWR. The WAMS may be utilized to obtain images for faster screening or identification of corrosion features on the surface while the LCM can be utilized to obtain higher resolution images of selected areas identified by the WAMS [3]. This report includes a summary of the data generated by WAMS in FY21. During this time the area where image was collected was increased to cover a larger region where cracks may develop in the ICCWR. Analysis of the data collected by WAMS is in progress, and the processed sample data is included. To determine the efficiency of the WAMS as compared to a lower-cost microscope, data generated by the WAMS is compared to that generated using a Dino-Lite Edge™ microscope.

2.0 Experimental Procedure

A complete analysis of the inner container closure weld region (ICCWR) on selected DE inner containers is in progress in collaborations with Los Alamos National Laboratory (LANL) and the Materials Identification and Surveillance (MIS) Working Group. Figure 1 summarizes the analysis process. It is described in more detail in the "Wide Area 3D Measurement System for Analysis of 3013 Inner Container Closure Weld Region" report (SRNL-STI-2020-00418) [3]. The document herein includes the WAMS data collection and analysis component of the protocol.

Data collection of the containers is being carried out by high resolution rapid imaging of sectioned DE containers using a Keyence VR-5000 Wide Area 3D Measurement System (WAMS) optical microscope. The WAMS wide area collection capability was utilized to carry out high resolution rapid imaging of the ICCWR samples. It is a 3D surface microscope, similar to the LCM, with capabilities to collect digital optical images and topographical data. A key difference is that the WAMS uses a white LED's as the light source compared to the LCM, which uses a monochromatic red laser light. Although at lower resolution than the LCM, the WAMS has the capability to measure broad areas with high accuracy and speed.

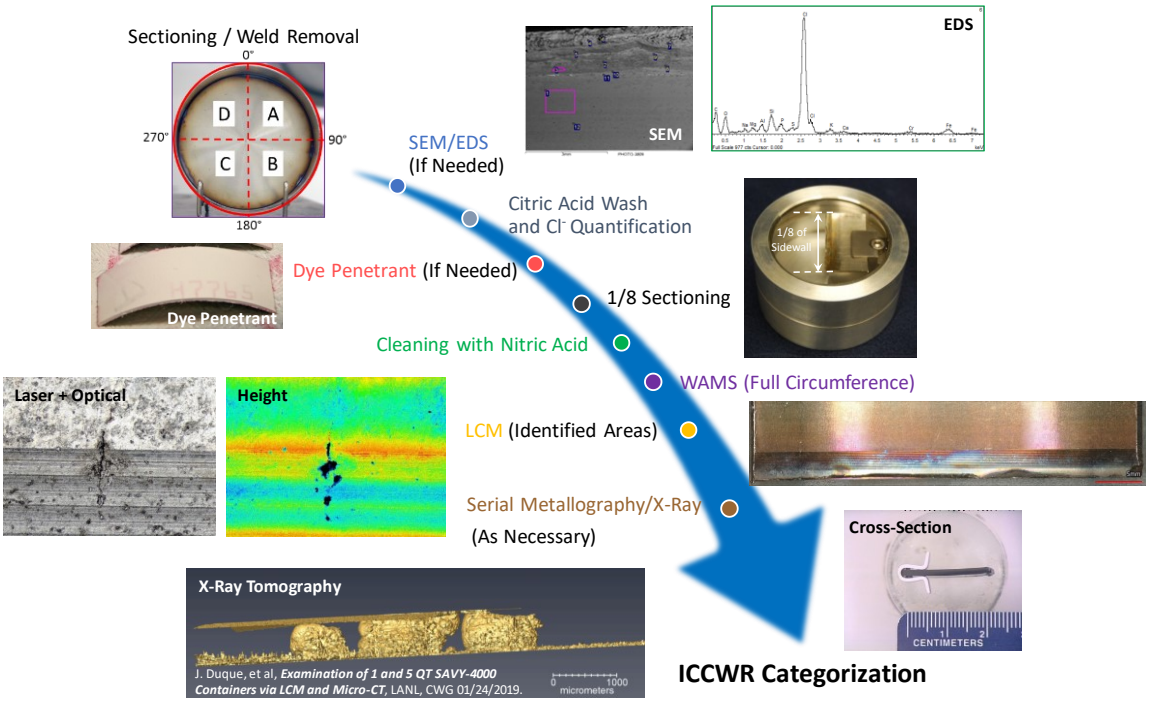

Figure 1. Protocol for the examination of the ICCWR [3, 4].

The objective of this work is to identify the occurrence of stress corrosion cracking and pitting of the inner surface of the cans within and near the heat affected Zone of the lid-weld-region of the inner-containers though WAMS data collection and micrograph analysis. Characterization analysis is in progress through manual examination of the generated micrographs by SRNL researchers to preliminarily identify features of concern for further analysis by LCM, and to provide a baseline analysis to support the development of automated computer analysis currently under development by LANL and the University of South Carolina researchers [7]. To aid the analysis, data is collected in monochrome and color images settings.

To obtain a comparison of image quality and efficiency for data collection, the WAMS data was compared to that on a low-cost Dino-Lite Edge (DLE) digital microscope. The DLE is a simple manually operated microscope.

3.0 Results and Discussion

Several DE containers were selected for characterization of the inner container closure weld region (ICCWR). The ICCWR was sectioned into 8 sample pieces (A1, A2, B1, B2, C1, C2, D2, and D2) that encompassed the full circumference of the can near the weld region. Some of the sample pieces were then selected for analysis with the WAMS. As of this writing, data has been collected on a total of 48 DE sections. Of these, 22 were collected during FY21.

Differing sections of the DE container near the weld region are defined as Zones 1 through 3 to distinguish areas of interest as shown in Figure 2. Zones 1 and 2 are defined by the topography of machining marks made during manufacturing. Note that in most DE samples, Zone-1 is covered by the weld or destroyed during preparation of the sample. Zone 3 is the unmachined inner surface area of the container's cylinder.

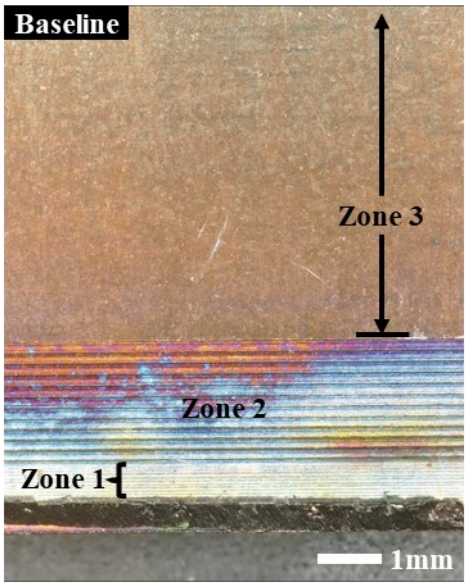

Figure 2. Defined areas for characterization of the DE samples.

During early characterizations, data was collected using a grid with one row of images that contained the areas of interest deemed necessary for analysis of the sample. This resulted in images that included Zone 1, if available, Zone 2 and a depth of approximately 3 mm into Zone 3 of the DE samples. With the introduction of the WAMS, the reduced scan area came as most major features were found in the Zone 2/3 boundary. However, concerns of missing features within the Zone 3 from the "already defined 6-mm threshold" [8] it was decided to expand the scanning area to the WAMS data as to match the LCM. Figure 3 shows a micrograph generated by the WAMS of a selected sample (FY17 DE04 A1) that is representative of the early high-resolution images generated during characterization. Figure 4 shows a micrograph generated by the WAMS that includes at least 6mm of Zone 3.

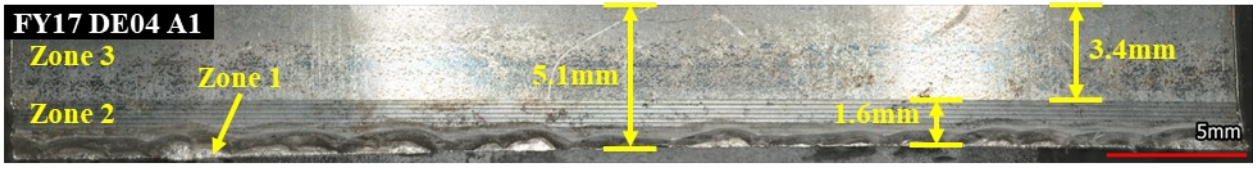

Figure 3. Early characterization areas displaying sample FY17 DE04 A1.

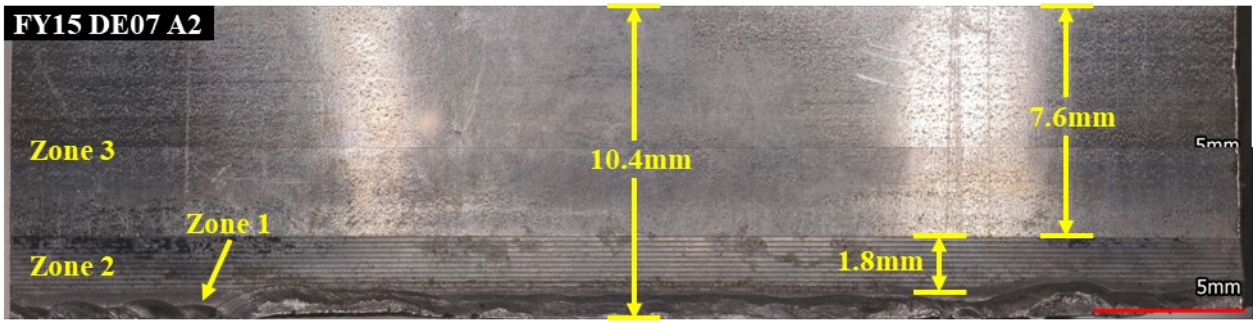

Figure 4. Sample FY15 DE07 A2 imaged to at least 6mm into Zone 3.

The WAMS collects data on a predetermined area with the number of frames in a grid specified by the researcher. The microscope automatically collects images on each grid section and automatically stiches the images together to produce a single high-resolution micrograph of the selected area of the sample. The microscope has a software-imposed image size limit of 25 megapixels (MP) per stitched image. If the selected grid results in an image that exceeds this limit, the microscope's software automatically reduces the image size to remain within the limit. This image reduction results in an undesired decrease in image resolution. During the high-resolution data collection process used to image the DE's, the collection grid is restricted to approximately eight frames before the stitched image exceeds 25 MP. The actual number of frames and image size depends on the amount of overlap that the unstitched images have that in turn depends on how the initial grid is overlayed onto the sample.

For the DE sections where data was collected to a distance of approximately 3 mm into Zone 3, the WAMS required 7 or 8 frames to image the sample from left to right in a single row. This permitted data collection of a DE section (e.g., A1, A2, B1, B2…) in a single step and produced micrographs with approximately 19 MP. To aid the image analysis in regions of high reflectivity, additional images were normally collected from these regions using lower light brightness settings to compensate for image saturation during automatic data collection. The images were either analyzed separately or were manually stitched to the parent micrograph for analysis.

Expansion of the data collection process to include at least 6 mm into Zone 3 requires collection of a second row of data, which results in approximately 14 to 16 data frames that exceed the 25 MP image limit. To produce micrographs without sacrificing resolution, the data collection process was modified to collected data using several data collection steps. This requires additional interactions of the researcher with the microscope and introduced a manual image stitching step but maintained the maximum resolution of the micrographs.

To collect at least 6 mm of Zone 3, initially the WAMS was setup so that two rows of images were collected from the DE in separate runs, as shown in Figure 5. This setup allowed for rapid data collection. However, the additional images that were required to compensate for the samples' reflectivity resulted multiple additional data collection steps. To optimize data collection times, the data collection process was modified to collect grids two rows vertically with one to four rows horizontally as shown in Figure 6. This permitted more efficient control over data collection in the highly reflective areas for most samples.

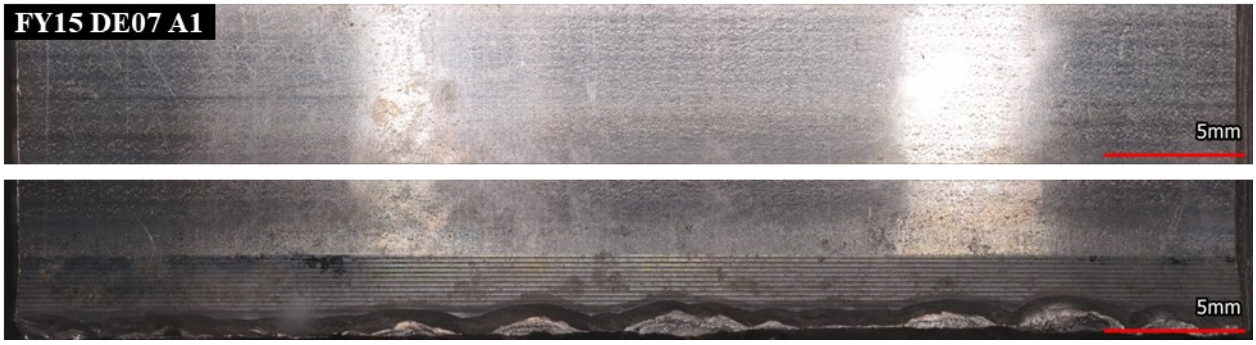

Figure 5. Two image datasets generated by the WAMS for manual stitching to produce a larger micrograph each composed of 1 X 7 (length X height) grids.

Figure 6. Three image datasets generated by the WAMS for manual stitching to produce a larger micrograph with a 1 X 2 grid for the left image, a 2 X 4 for the center image, and a 2 X 2 for the right-side image.

Table 1 shows a complete list of the samples where data was collected by WAMS up to the end of FY21. The corresponding micrographs are shown in Appendix A. The table differentiates between samples where data was collected to 3 mm and 6 mm into Zone 3 and includes a list of samples that have undergone additional characterization in the LCM. The samples scheduled for data collection in FY21 were completed, and data was generated on:

- FY11 DE13: C1 and C2
- FY15 DE06: A1, A2, B1, B2, C1, C2, D1, and D2
- FY15 DE07: A1 and A2
- FY16 DE02: A1, A2, B1, B2, C1, C2, D1, and D2
- FY16 DE05: B2 and D1

Table 1. DE container characterization status.

DE	LCM (6mm in Zone 3)	WAMS (3mm in Zone 3)	WAMS (6mm in Zone 3)
FY11 DE13 (HHMC)	B1, B2, B3	A1, A2, C1, C2, D1, D2	
FY15 DE06			A1, A2, B1, B2, C1, C2, D1, D2
FY15 DE07	A1, A2, B1, B2, C1, C2, D1, D2	C1, C2	A1, A2
FY15 DE08	A1, A2, B1, B2, C1, C2, D1, D2	B2, C2, D2	
FY16 DE02			A1, A2, B1, B2, C1, C2, D1, D2
FY16 DE05	A1, A2, B1, B2, C1, C2, D1, D2	C2b	B2, D1
FY17 DE04		A1, A2, B1, B2, C1, C2, D1, D2	
FY18 DE03		A1, A2, B1, B2, C1, C2, D1, D2	

Analysis of the samples using the micrographs generated by the WAMS is carried out manually. The micrographs are inspected in detail through careful visual examination of the color and the equivalent monochrome micrographs. To identify cracks, typically color and monochrome images are compared to determine if a given observed feature can be tentatively identified as a SCC on the surface of the sample. Figure 7 shows a selected area of sample FY17 DE04 B1 with eleven potential cracks marked by yellow rectangles in (a) the color and (b) the monochrome micrographs. This section appears to have developed very thin cracks that may be finer than the resolution of the microscope. Note that the identified cracks are barely discernable on either micrograph. Setting of the images to their full size or larger on a computer screen along with superimposition of the images results in better image acuity that permits a more reliable determination. Analysis of the collected data is currently in progress. Samples where the micrographs have been examined to identify suspect SSC cracks are highlighted with green text in Table 1. The marked micrographs of these analyzed samples can be found in Appendix B below.

Analysis of the samples showed that each sample developed large numbers of cracks and pits.

Table 2 summarizes the analysis results in terms of the number of cracks and pits observed. The analysis to date was concerned with identifying all the observed potential cracks and pits in order to aid automated analyzes in progress elsewhere. Note that higher uncertainty is present in the analysis for cracks that are near or finer than the pixel resolution of the microscope (3.7 μm/pixel), as these cracks typically appear blurred in the micrographs. A best judgment is made on these based on their observed morphology. Cracks and pits were observed distributed throughout the samples. Generally, higher densities of cracks and pits were observed in Zone 2 and in Zone 3 near to the Zone 2 and Zone 3 interface.

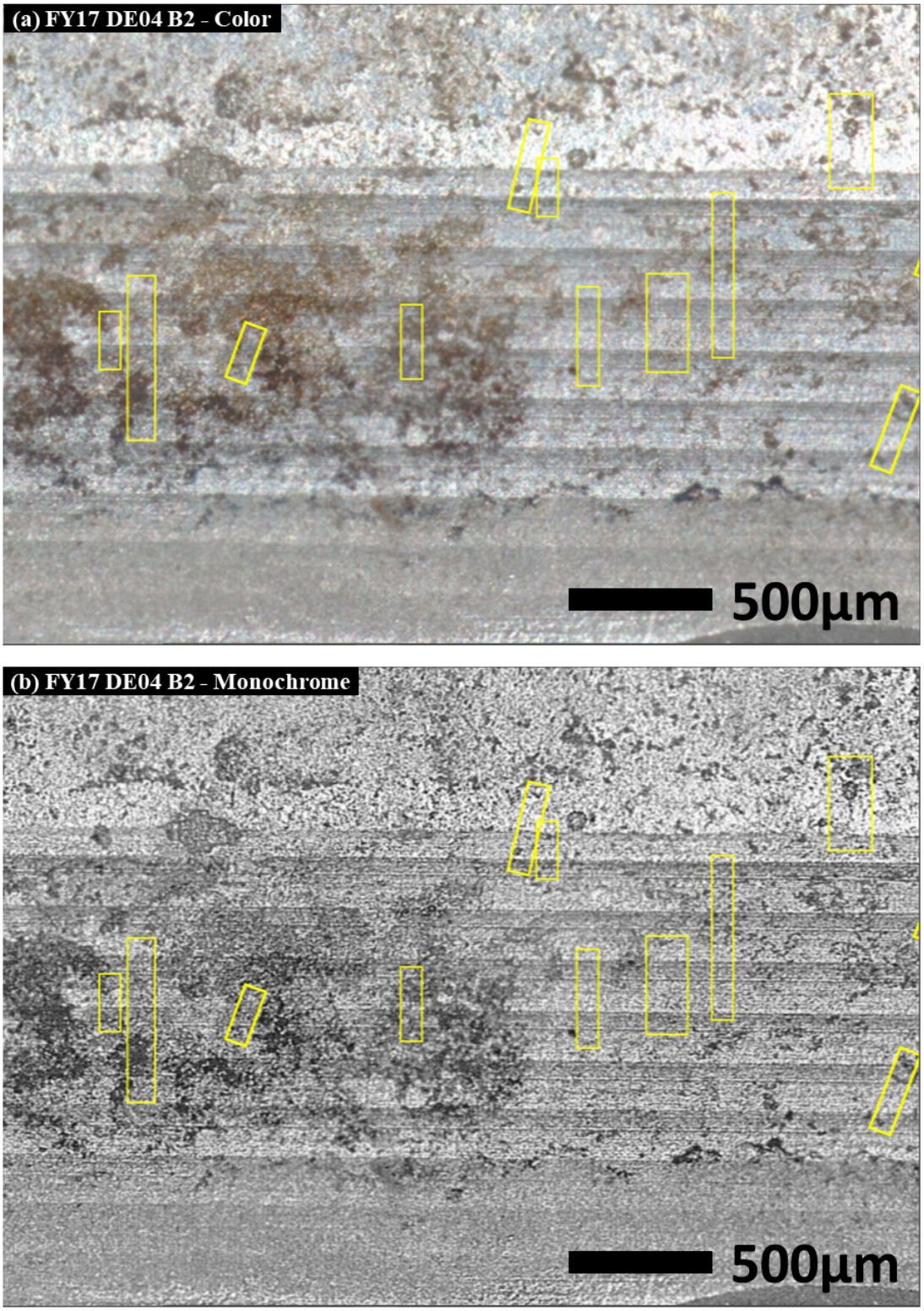

Figure 7. A section of sample FY17 DE04 B2 showing potential cracks near the interface in Zone 2 and at the Zone 2 and Zone 3 interface.

Table 2. Summary of the analysis results of the characterized samples.

DE	A1	A2	B1	B2	C1	C2	D1	D2
	(Cracking, Pitting)							
FY15 DE07					35, 28	65, 43		
FY15 DE08				89, 3		80, 23		102, 42
FY16 DE05				139, 49		(C2b) 48, 13		
FY17 DE04	79, 28	67, 25	80, 19	118, 25				

To develop a better understanding of the quality and efficiency of the WAMS microscope, it was compared with the simpler Dino-Lite Edge (DLE) digital microscope, model number AM7115MZTW, shown in Figure 8. The DLE is a commercial readily available microscope with 5MP image size (2592 X 1944 pixels) and a wide field-of-view with a magnification range of 10X - 50X. It collects individual images without an option in the included software to stitch images.

Figure 8. Dino-Lite Edge digital microscope model number AM7115MZTW.

To provide a relevant comparison, sample FY15 DE06 C1 was imaged with the WAMS and the DLE as shown in Figure 9. The WAMS image is a composite of 14 individual frames. Prior to stitching each WAMS image is 3MP (2048 X 1537 pixels) and has a resolution of 3.7 μm/pixel at the chosen magnification. The DLE image in Figure 9 is composed of 7 frames. To collect the DLE micrographs, the microscope was fixed on a standard laboratory stand. The DLE magnification and focus are linked through its focal length; focusing on a given area affects the magnification. Thus, a magnification was chosen so that the DLE images appeared to have a similar magnification to that of the standard WAMS images. This setup resulted in and image resolution of 3.1 μm/pixel for the DLE.

The microscope was then fixed in place at the determined focal length to collect images of the full DE sample. To compensate for the curvature of the sample and the focal point at the given magnification, the

microscope was physically moved up or down on the stand prior to collecting each image to focus the microscope. This procedure presented a challenge in terms of maintaining the alignment of the microscope with the sample. Images were collected as best as the sample could be realigned with the microscope for each image. As can be seen in Figure 9 (b) the alignment efforts were not ideal. Better alignment may be achieved by placing a moving stage under the microscope in lieu of manual handling. To produce the stitched micrograph, the individual images were then manually stitched using PowerPoint. During the stitching process, however, image edge aberrations were observed that did not permit precise image matching.

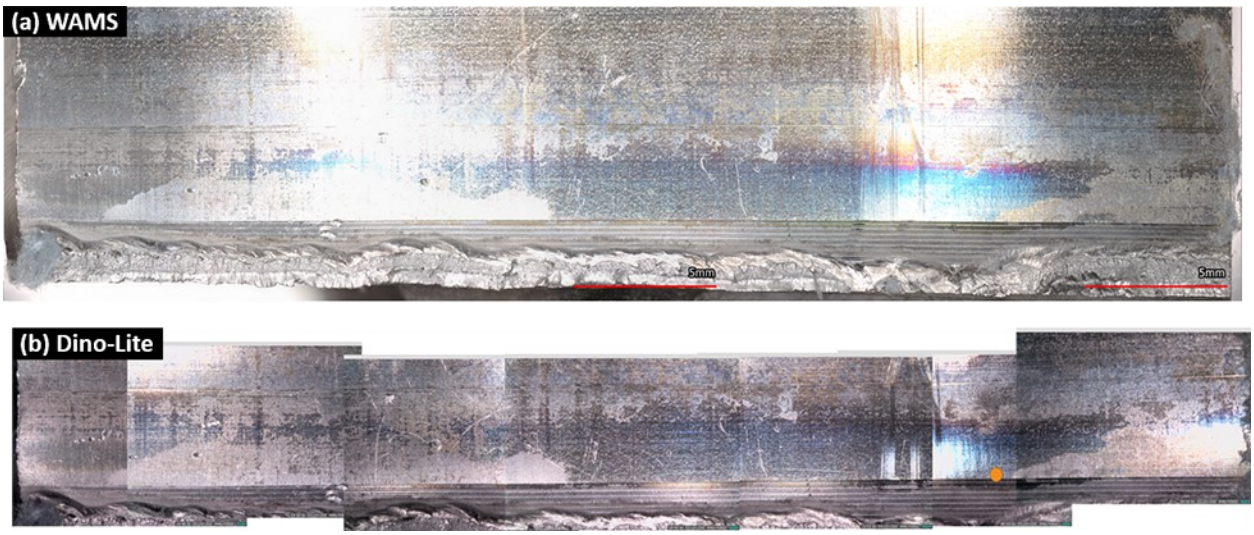

Figure 9. Optical micrographs of sample FY15 DE06 C1 collected using (a) the WAMS and (b) the DLE.

At lower magnification as shown in Figure 9, the images appear to display equivalent details. Note that some color differences are evident; however, this does not appear to affect the image details from the surface features of the sample. Figure 10 shows low and higher magnification micrographs of a selected section of sample FY15 DE06 C1 for the WAMS and the DLE. The low magnification micrographs (a) and (b) were taken from the leftmost frames from the WAMS and DLE micrographs in Figure 9, but Figure 10 displays the section with greater detail. This section was chosen because the curvature of the sample has the greatest effect on imaging focusing near the left and right edges of the DE samples. At the magnification in Figure 10 (a) and (b) both micrographs still appear nearly equivalent in terms of focusing.

Higher magnification micrographs are shown in Figure 10 (c) and (d). These micrographs were selected to include several potential cracks that were observed in the WAMS micrograph. The images in (c) and (d) present the same section of the sample. The cracks widths as seen in the WAMS micrograph were approximately 1 to 4 pixels thick. This is equivalent to approximately 3.7 μm or thinner to 14 μm thick. A more precise measurement was not possible due to the resolution limit of the micrograph. At this higher magnification significant differences became evident. Although the DLE micrograph contains a higher pixel resolution than the WAMS micrograph, 3.1 μm/pixel vs. 3.7 μm/pixel (larger pixels result in lower resolution), sharp image focus at this magnification was not achievable with the DLE. The area selected in Figure 10 (c) and (d) was also chosen because the section showed the best focused area of the DLE micrograph.

The WAMS microscope produces a fully focused image through automatic collection of several images focused at varying heights, discarding of the unfocused areas, and final reconstitution of the original imaged area. Furthermore, it can then collect several areas in a grid pattern to generate a single large stitched and

fully focused micrograph. It possesses very low aberration lenses, and it can collect on data automatically complex shapes at high speeds. Additionally, it collects detailed topographical (height and width) data of objects under study to produce 3D reconstructions of the object under study.

The DLE microscope, on the other hand, is focused manually, can only focus on a spot in the area under study, and the focal point and magnification are coupled (focusing adjustments change the magnification). During image collection, the DLE was focused on the center of the visible area of the sample. The area selected in Figure 10 (d) is near the center of the generated DLE micrograph. Due to the curvature of the sample, the area to the left of the focal point would then experience an underfocused condition and that to the right would be in an overfocused condition. This setup permits the capture of an image with a continuous focal-gradient from underfocused to fully focused to overfocused states. The micrograph then contains an area of maximum focus, regardless of possible misfocus by the operator. Examination of the DLE micrograph showed that the area of maximum focus in the micrograph in Figure 10 (b) and (d) was near the center of the micrograph in the area shown in (d). This demonstrated that the DLE microscope at higher image zooms was not able to produce a clearly focused image comparable to those from the WAMS. Testing of the DLE at higher magnifications was not attempted because the increased cost due to the increased complexity of collecting focused and aligned images manually outweighs any cost savings that could conceivably be achieved by acquiring and/or using the DLE microscope.

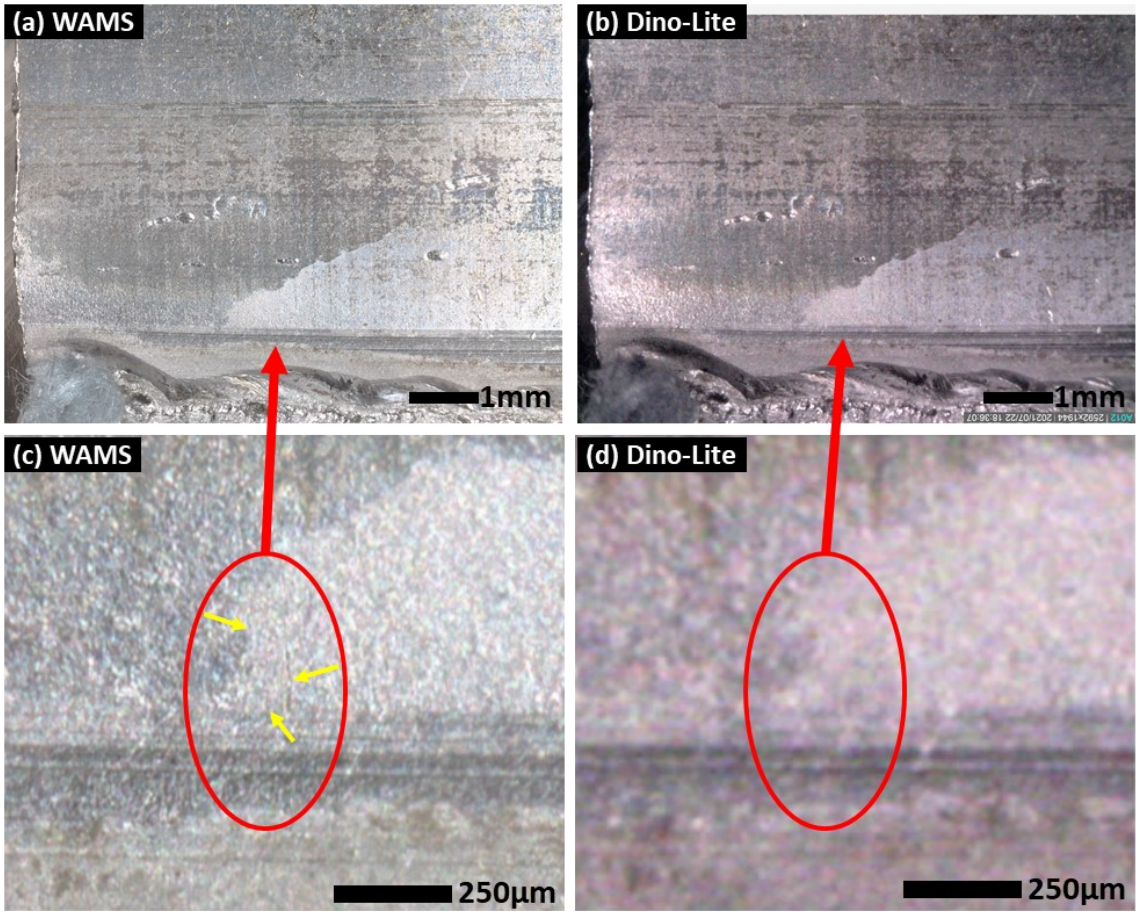

Figure 10. Comparisons between the WAMS and the DLE at low and higher magnifications.

4.0 Summary

The WAMS microscope has been successfully used to image ICCWR DE samples. The generated data, although with lower resolution than the LCM, can be used to identify potential cracks and pitting of the samples. Data was successfully collected in 22 DE samples, and analysis has been completed for 11 samples. Although uncertainty in the analysis of fine crack is high, analysis of the WAMS micrographs showed that each DE sample developed a large number of cracks and pits distributed throughout the samples' surfaces. Crack and pit density appeared to be higher on the areas near the interfaces between Zones 2 and 3.

Comparison with the DLE microscope established that the WAMS collects superior well focused images that permit more detailed analysis of the samples' surfaces. At identical high magnifications the DLE micrographs were sufficiently out of focus to prevent detailed analysis. The difficulties of working with the DLE setup effectively result in higher operational costs that outweigh the initial cost savings of purchasing the DLE.

5.0 Recommendations, Path Forward or Future Work

- Data collections and analysis with the WAMS will continue until determined otherwise.
- WAMS data will be directly compared to LCM data for further validation of the collection process.
- Data collection via electron microscopy should be attempted to determine if better analysis efficiencies can be achieved.

6.0 References

1. Berg, J.M., D.K. Veirs, E.J. Kelly, Juan G. Duque, S.A. Joyce, J.E. Narlesky, J.M. Duffey, J.I. Mickalonis, and K.A. Dunn, "Test Plan for Assessing Potential for Stress Corrosion Cracking in the 3013 Inner Container Closure Weld Region (FY 2014)," 2014, LA-UR-14-20785.

2. Martínez-Rodríguez, M.J., "Laser Confocal Microscope for Analysis of 3013 Inner Container Closure Weld Region," 2017, SRNL-STI-2017-00589.

3. Martínez-Rodríguez, M.J., "Wide Area 3D Measurement System for Analysis of 3013 Inner Container Closure Weld Region," 2020, SRNL-STI-2020-00418.

4. Michael J. Martínez-Rodríguez, Emmanuel E. Pérez, "2019 Destructive Evaluation and Inner Container Closure Weld Region Microscopy Observations," 2020, SRNL-STI-2020-00033.

5. Martínez-Rodríguez, M.J., "Status of the Full Circumference Examination of the Inner Container Closure Weld Region for Selected 3013 DE Containers," 2018, SRNL-L4400-2018-00017.

6. Emmanuel Pérez, Michael J. Martínez-Rodríguez, Torrian Walker, Joe Smith, Beth Lewczyk, Kellie Holland, Lisa Ward, and Gregg Creech, "ICCWR Analysis by WAMS and LCM," 2021, SRNL-STI-2021-00087.

7. Bruce Hardy, Anna d'Entremont, Jason Bakos, Taylor Clingenpeel, Michael Martínez-Rodríguez, Brenda García-Díaz, "FY20 Progress Report: SRNL Analysis of ICCWR LCM and WAMS data for Corrosion and Cracking," 2020, SRNL-STI-2020-00355.

8. Martínez-Rodríguez, M.J., Laser Confocal Microscope for Analysis of 3013 Inner Container Closure Weld Region, SRNL-STI-2017-00589 (2017).

Appendix A: Micrographs of the DE samples collected in FY21


FY11 DE13 C1
5mm
FY11 DE13 C2
5mm
FY15 DE06 A1


FY15 DE06 A2


FY15 DE06 B1


FY15 DE06 B2
5mm


FY15 DE06 C1
5mm

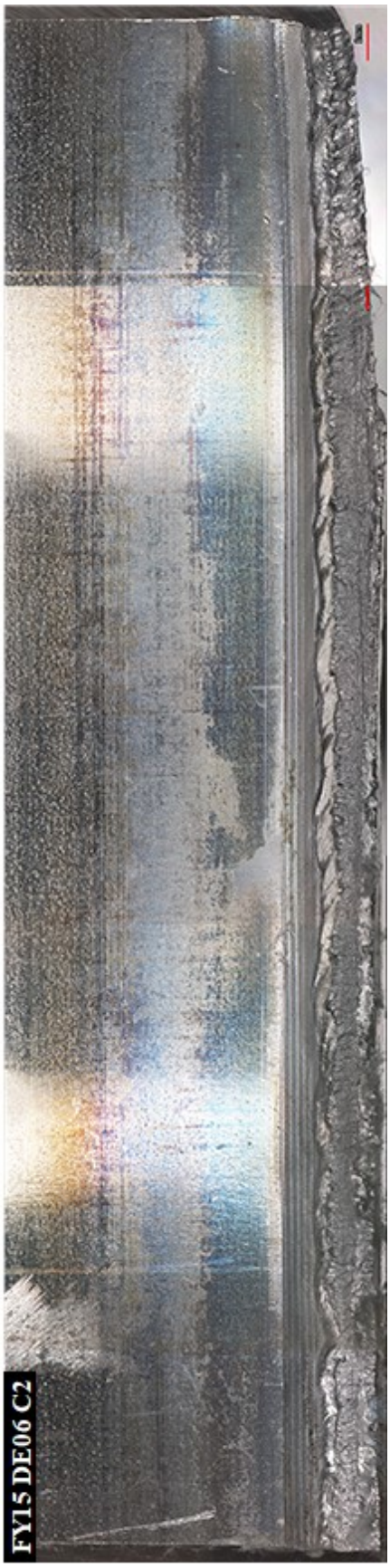
FY15 DE06 C2


FY15 DE06 D1


FY15 DE06 D2
5mm


FY15 DE07 A1
5mm
5mm

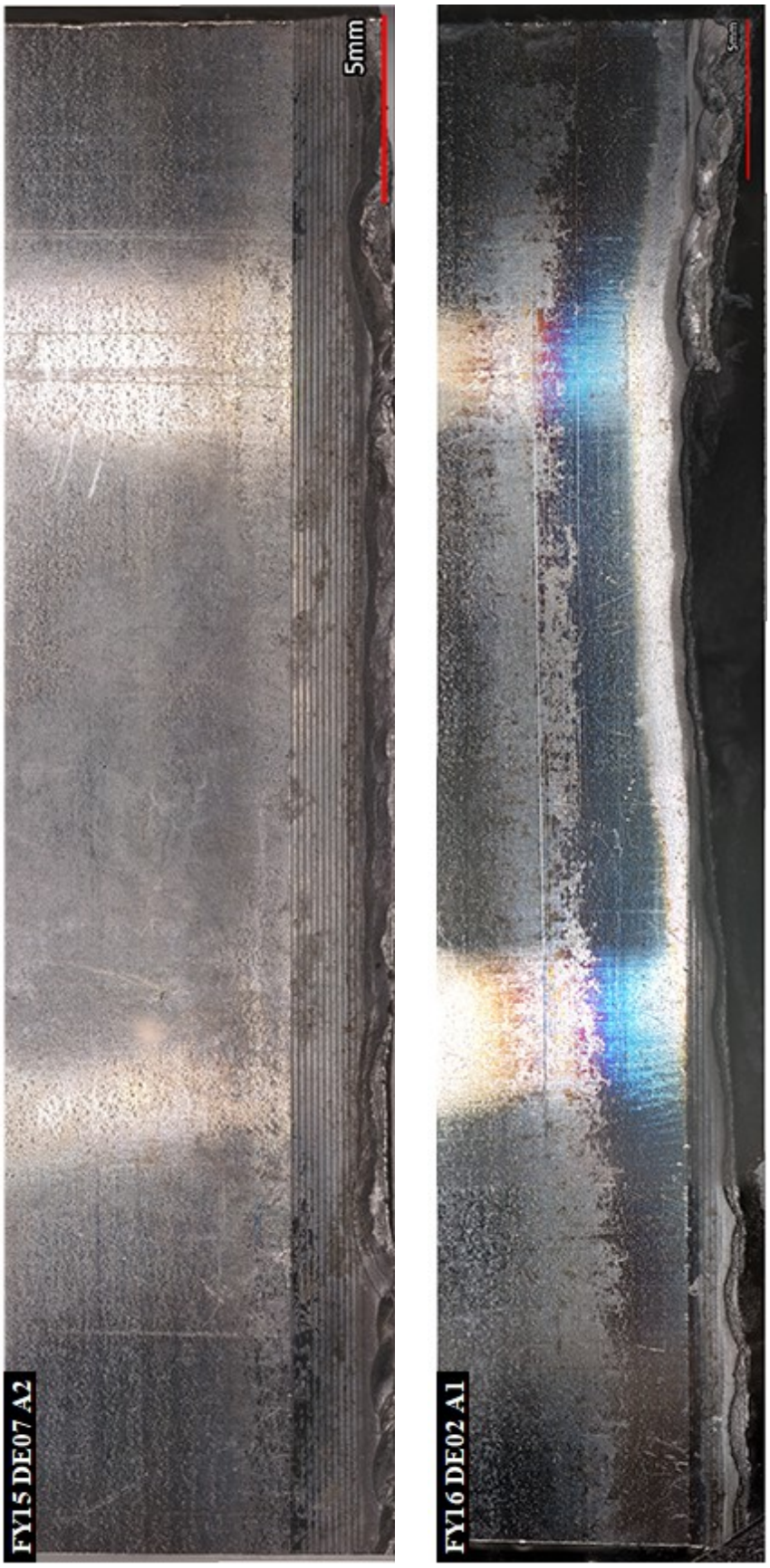
FY15 DE07 A2
5mm
FY16 DE02 A1


FY16 DE02 A2


FY16 DE02 B1
5mm


FY16 DE02 B2


FY16 DE02 C1

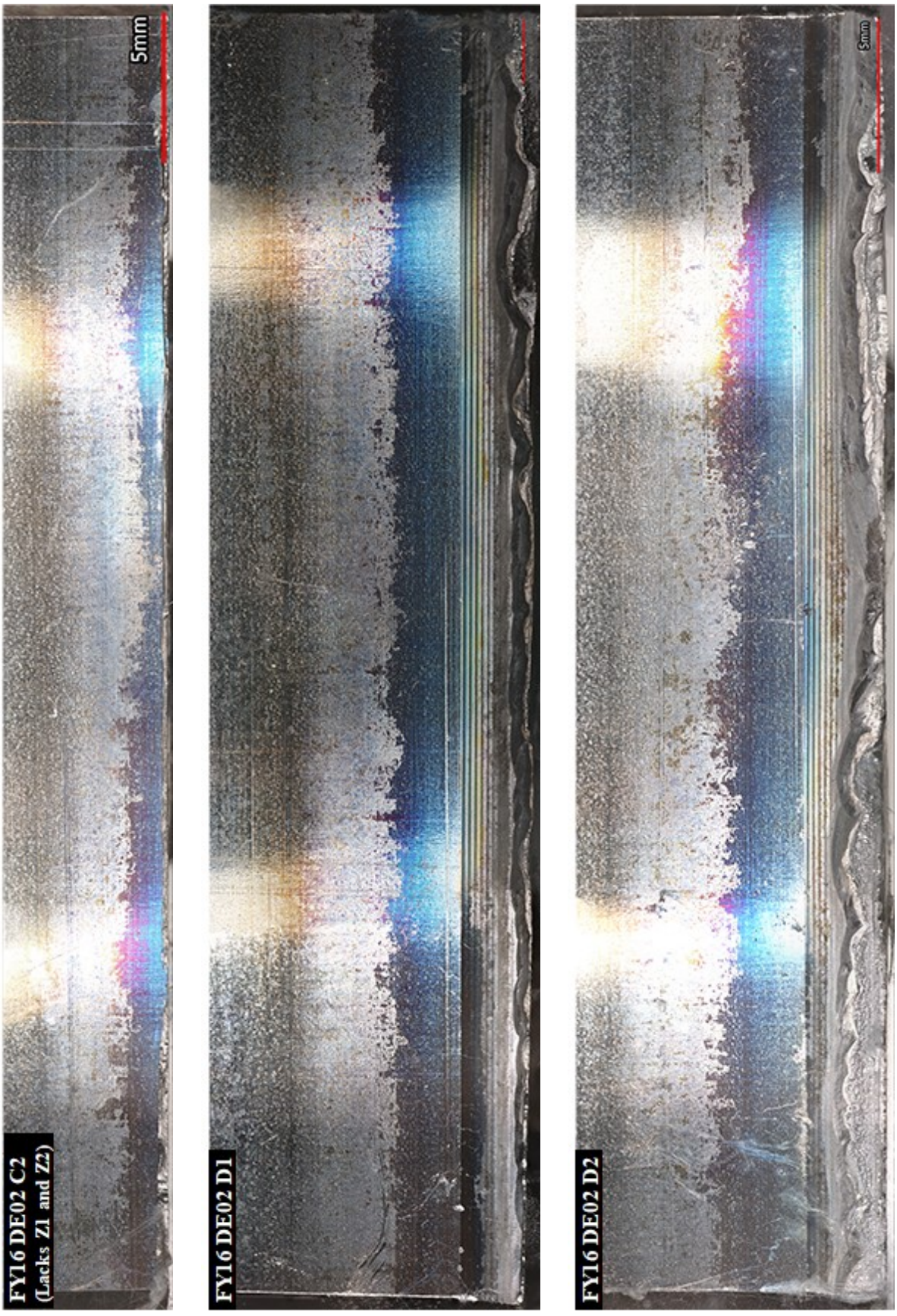
FY16 DE02 C2
(Lacks Z1 and Z2)
5mm
FY16 DE02 D1
FY16 DE02 D2
5mm

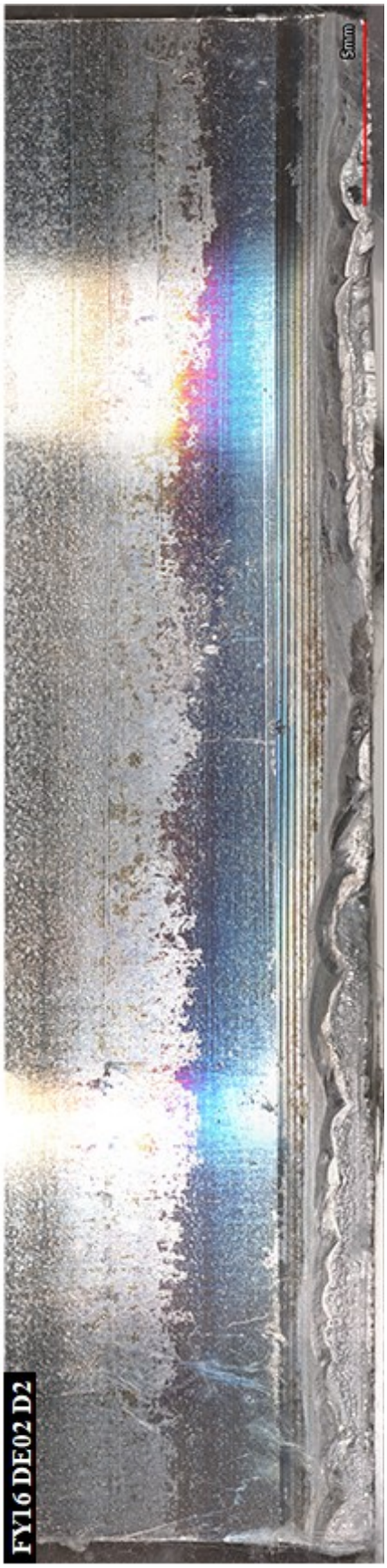
5mm
FY16 DE02 D2


5mm
FY16 DE05 D1

Appendix B: Annotated Micrographs of the DE samples

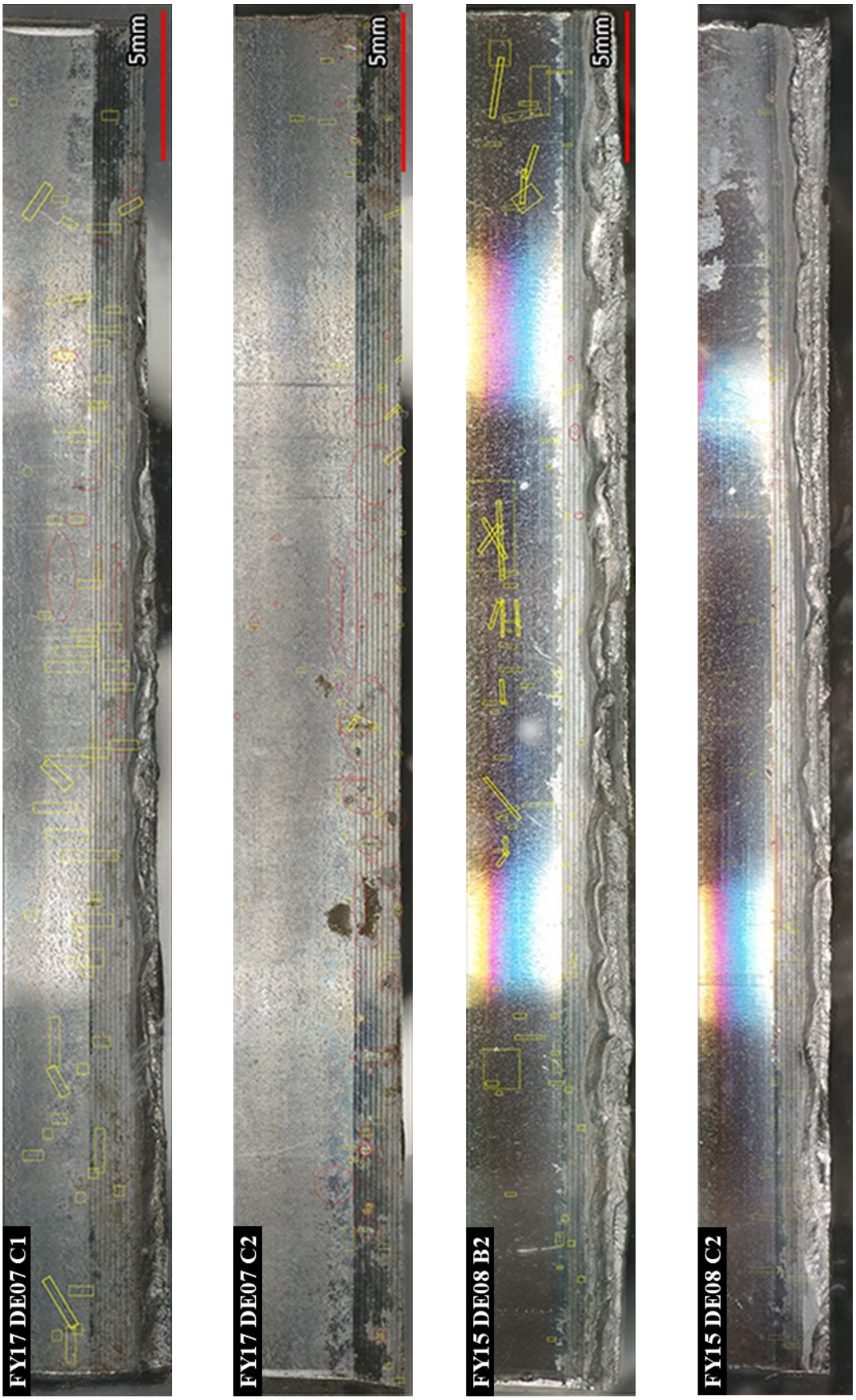
5mm
FY17 DE07 C1
5mm
FY17 DE07 C2
5mm
FY15 DE08 B2
FY15 DE08 C2

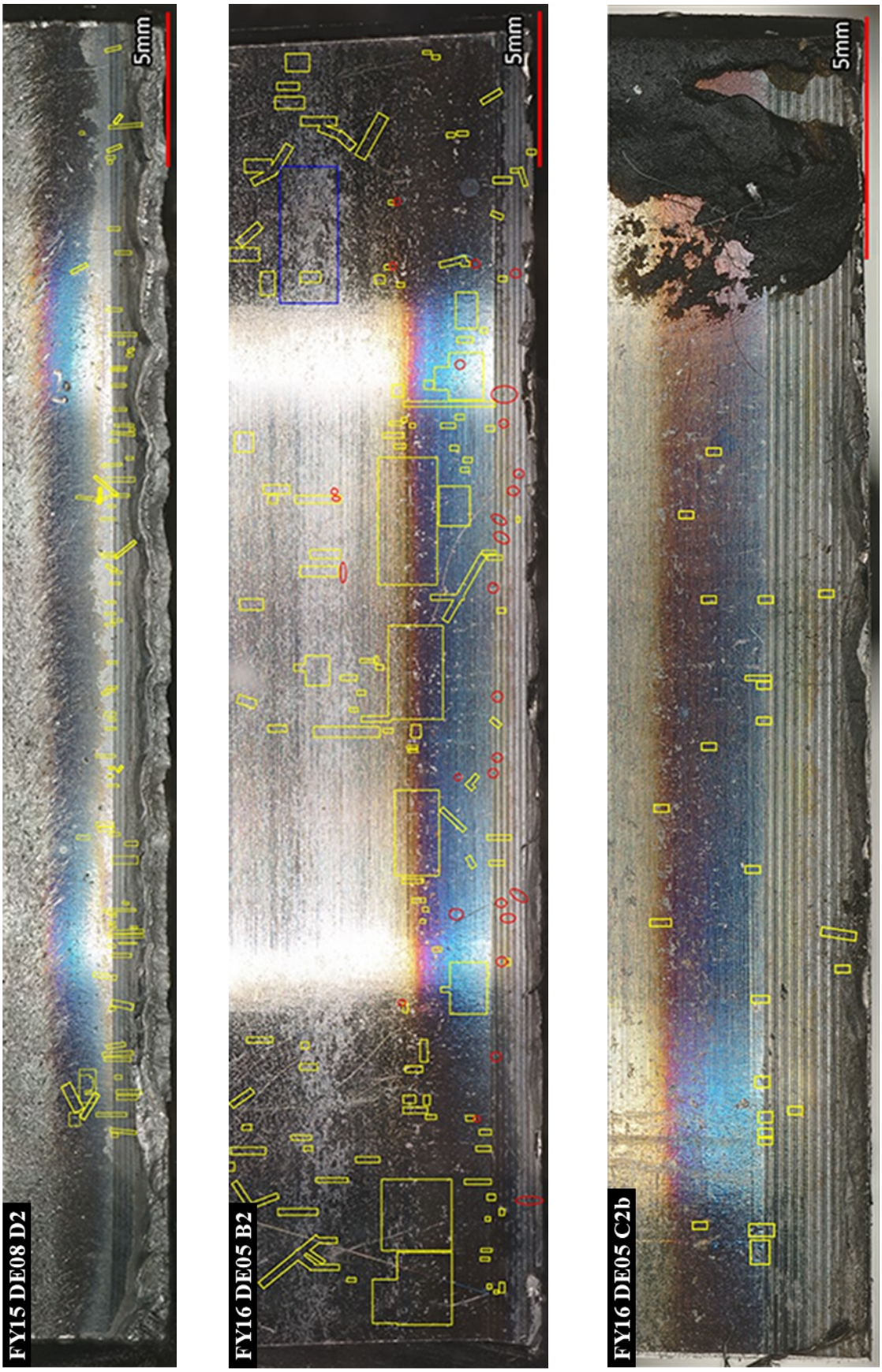
FY15 DE08 D2
5mm
FY16 DE05 B2
5mm
FY16 DE05 C2b
5mm

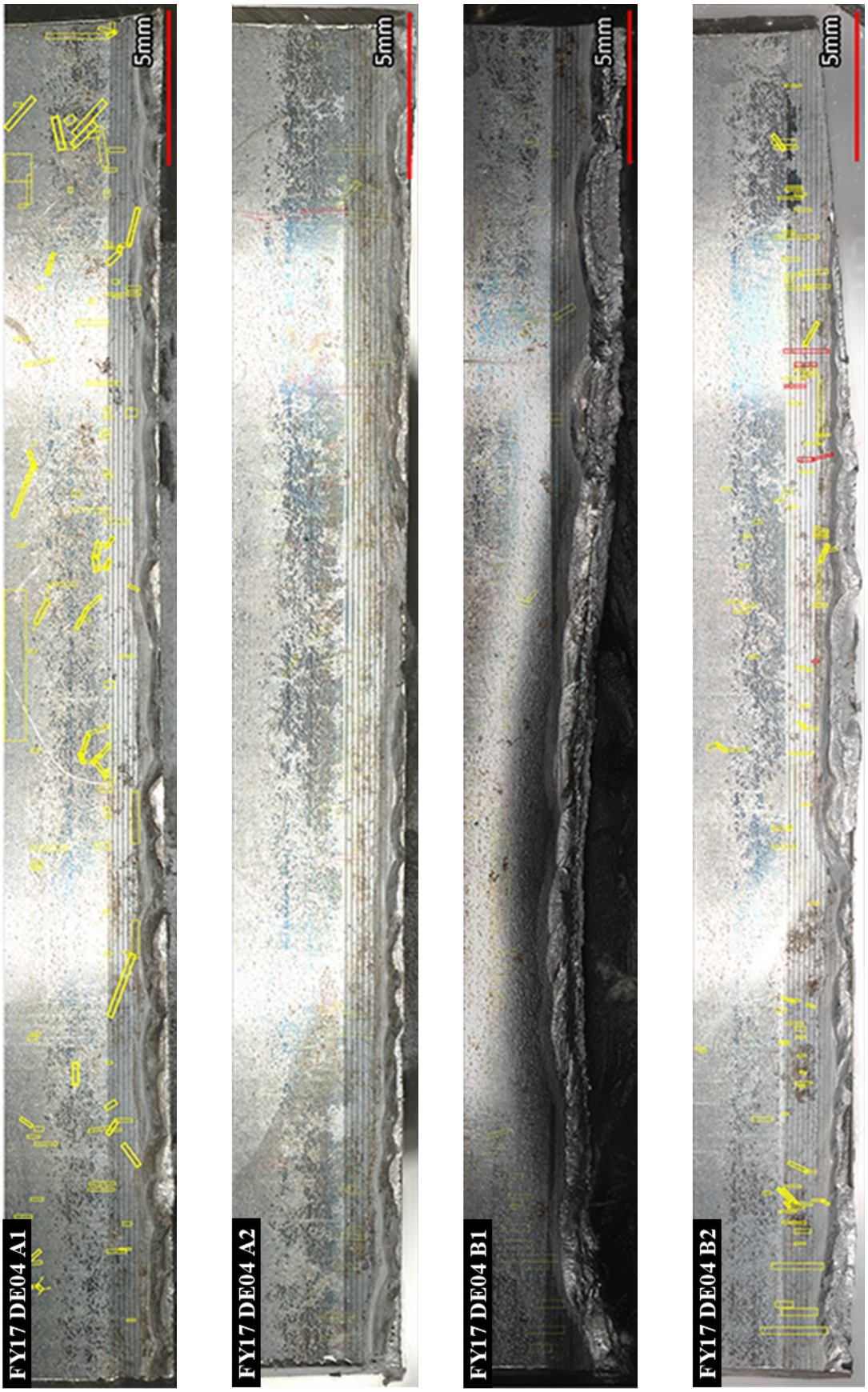
5mm
FY17 DE04 A1
5mm
FY17 DE04 A2
5mm
FY17 DE04 B1
5mm
FY17 DE04 B2